Modifications to Kozeny-Carman Model to Enhance Petrophysical Relationships

Amir Maher Sayed Lala

Geophysics Department, Ain Shams University

e-mail: amir77_lala@yahoo.com

Affiliation: Geophysics Department, Fac. of Science, Ain Shams University, Cairo, Egypt

Abstract

The most commonly used relationship relates permeability to porosity, grain size, and tortuosity is Kozeny-Carman formalism. When it is used to estimate the permeability behavior versus porosity, the other two parameters (the grain size and tortuosity) are usually kept constant. Here, we investigate the deficiency of the Kozeny-Carman assumption and offer alternative derived equations for the Kozeny-Carman equation, including equations where the grain size is replaced with the pore size and with varying tortuosity. We also introduced relationships for the permeability of shaly sand reservoir that answer the approximately linear permeability decreases in the log-linear permeability-porosity relationships in datasets from different locations.

Introduction

Darcy's law (e.g., Mavko et al., 2009) states that, the volumetric flow rate of viscous fluid Q (volume per time unit, e.g., m^3/s) through a sample of porous material is proportional to the cross-sectional area A and the pressure difference ΔP applied to the sample's opposite faces, and inversely proportional to the sample length L and the fluid's dynamic viscosity μ, as shown as follows:

$$Q = -k\frac{A}{\mu}\frac{\Delta P}{L} \quad (1)$$

The proportionality constant k is called the absolute permeability. The main assumption of Darcy's law is that, k does not depend on the fluid viscosity μ or pressure difference ΔP and assume a laminar fluid flow and is valid under a limited range of low velocities. All inputs in equation 1 have to be consistent units, meaning that if length is in m, pressure has to be in Pa and viscosity in Pa s. The most commonly used viscosity unit is cPs = 10^{-3} Pa s. It follows from Equation 1 that the units of k are length squared, e.g., m^2. The most common permeability units used in the industry are Darcy (D) and/or

milliDarcy (mD): 1D = 10^{-12} m^2 and 1 mD = 10^{-15} m^2. In many cases the fluid flow is not laminar and permeability requires a correction for the Forchheimer and/or Klinkenberg effect. Forchheimer effect also known as non-Darcy effect is very important for describing additional pressure drawdown due to high fluid flow rates and could reduce the effective fracture conductivity and gas production (Guppy et al., 1982; Katz and Lee, 1990; Matins et al., 1999; Garanzha et al., 2000). Permeability is a fundamental rock property and remains constant, so long as the sample microstructure is unchanged – this is the reason that permeability is independent of the fluid type and the pressure conditions.

The Kozeny-Carman (KC) formalism (e.g., Kozeny, 1927; Carman, 1937; Guéguen and Palciauskas, 1994; Mavko et al., 2009; Bernabé et al., 2010) assumes that a porous solid can be represented as a solid block permeated by parallel cylindrical pores (pipes) whose axes may be at an angle to the direction of the pressure gradient, so that the length of an individual pipe is larger than that of the block. To relate permeability to porosity in such idealized porous solid we need to find how the volumetric flow rate Q relates to the pressure gradient ΔP. The solution is based on the assumption that each cylindrical pipe is circular, with radius r. The Navier-Stokes equations governing laminar viscous flow through a circular pipe of radius r provide the following expression for the volumetric flow rate Q through an individual pipe:

$$Q = -\frac{\pi r^4}{8\mu}\frac{\Delta P}{l} \qquad (2)$$

where: l is the length of the pipe.

Our derivation starts from the Kozeny-Carman equation by assuming that a rock includes porosity of pipe shape. The porosity, φ, and the specific surface area, S, can

be expressed in terms of the properties of the pipe by the following relations (Mavko et al., 2009):

$$\varphi = {\pi r^2 l}/{AL} = {\pi r^2}/{A}\,\tau \quad \ldots\ldots (3)$$

Where τ is the tortuosity (defined as the ratio of total flow path length to length of the sample) .

$$S = {2\pi r l}/{AL} = {2\pi r \tau}/{A} = {2\pi r^2 \tau}/{A}\,{2}/{r} = {2\varphi}/{r} \quad \ldots\ldots (4)$$

Permeability of this rock is expressed by its porosity φ and the specific surface area *S*, its length, and the number of the pipes, and using Equation 1 and 2, we get:

$$k = {\pi R^4}/{8A}\,{L}/{l} = {\pi R^4}/{8A\tau} = \frac{1}{2}\frac{\varphi^3}{S^2\tau^2} \quad \ldots\ldots (5)$$

where: *S* is defined as the ratio of the total pore surface area to the total volume of the porous sample and the tortuosity τ is simply l / L , defined as the ratio of the length of the fluid path to that of the sample. Porosity can be evaluated in the laboratory or obtained from porosity logs. The specific surface area is much more difficult to measure or infer from the porosity because the granular pore spaces geometry is not consistent with the pipe like geometry model of the original K-C functional form. One other parameter that can be determined in the laboratory by sieve analysis or optical microscope is the average grain size (diameter) d. The sieve analysis is the most easily understood laboratory method of determination where grains are separated on sieves of different sizes. This is why it is possible to conduct relationship between *k* and d. So modified Kozeny– Carman equation is needed if a non-fractal spherical grain packing model is assumed (yielding a constant tortuosity) and the effective pore radius is substituted by a term involving the specific surface expressed by the grain radius and the porosity. This operation is inconsistent with the KC formalism but it is useful. Assume that the number of these spherical grains is n, their volume is $n\pi d^3 / 6$ while

their surface area is $n\pi d^2$. Because the grains occupy the volume fraction 1-φ of the entire rock, the total volume of the rock is $n\pi d^3 / 6(1-\varphi)$. As a result, the specific surface area is $6(1-\varphi) / d$.

By replacing *S* in equation 3 with the latter expression, we find:

$$k = \frac{d^2}{72\tau^2}\frac{\varphi^3}{(1-\varphi)^2} \quad \ldots\ldots (4)$$

which is a commonly used form of KC equation (Mavko et al.,2009). The units used in this equation have to be consistent. In practical use they are often not, meaning that *d* is measured in mm while *k* is in mD. For these units, equation 4 can be read as:

$$k = 10^9\frac{d^2}{72\tau^2}\frac{\varphi^3}{(1-\varphi)^2} \quad \ldots\ldots (5)$$

Mavko and Nur (1997) modified this equation by introducing the percolation porosity φ_p below which the pore space becomes disconnected and *k* becomes zero, although φ is still finite:

$$k = 10^9\frac{d^2}{72\tau^2}\frac{(\varphi-\varphi_p)^3}{(1-\varphi+\varphi_p)^2} \quad \ldots\ldots (6)$$

where, as before, *k* is in mD, *d* is in mm, and φ is in fraction of one.

Kozeny-Carman Equation with Pore Size

As we discussed in the introduction, using the grain size in KC equation is not consistent with the formalism where the pore space is idealized as a set of parallel pipes.

Let us explore whether we can introduce the length parameter into KC equation in a more logical way and reformulate it using the pore size rather than grain size. With this goal in mind, let us recall another form of KC equation (e.g., Mavko et al., 2009)

$$k = r^2\frac{\varphi}{8\tau^2} = D^2\frac{\varphi}{32\tau^2} \quad \ldots\ldots (7)$$

where *r* is the radius of the circular pipe that passes through the solid block and *D* is its diameter.

Let us assume, hence, that the porosity only depends on the size of the pipe and is proportional to its cross-section, i.e., proportional to D^2. Hence, if the pore's diameter is D_0 at porosity φ_o and D at porosity φ,

$$\frac{\varphi}{\varphi_0} = \frac{D^2}{D_0^2}, D^2 = D_0^2 \frac{\varphi}{\varphi_0} \ldots\ldots\ldots\ldots\ldots\ldots\ldots\ldots\ldots\ldots\ldots (8)$$

As a result, by combining Equations (7) and (8), we obtain:

$$k = D^2 \frac{\varphi}{32\tau^2} = \frac{D_0^2}{\varphi_0} \frac{\varphi^2}{32\tau^2} \ldots\ldots\ldots\ldots\ldots\ldots\ldots\ldots\ldots\ldots\ldots (9)$$

This equation relates the permeability to porosity squared rather than cubed, the latter as in more common forms of the KC equation (equation 5). As a result, if in equation 9 we assume τ constant, the permeability reduction due to reducing porosity will be much less pronounced than exhibited by the Rudies Formation data obtained from Belayim marine field, Gulf of Suez, Egypt and the respective theoretical curves according to equation 6 and presented in figures 1 and 2, will strongly overestimate the permeability data. To mitigate this effect, let us assume that the tortuosity is not constant but rather changes with porosity.

The tortuosity is an idealized parameter that has a clear meaning within the KC formalism but becomes fairly nebulous in a realistic pore space that is not made of parallel cylindrical pipes. Still, numerous authors discussed the physical meaning of tortuosity in real rock, designed experimental and theoretical methods of obtaining it, and suggested that τ could be variable (even within the same dataset) as a function of porosity.

Let us focus here on two tortuosity equations:

$$\tau = \varphi^{-1.2}, \ldots\ldots\ldots\ldots\ldots\ldots\ldots\ldots\ldots\ldots\ldots (10)$$

That is derived from laboratory contaminant diffusion experiments by Boving and Grathwohl

(2001) and

$$\tau = {(1+\varphi^{-1})}/{2} \quad \ldots \quad (11)$$

That is theoretically derived by Berryman (1981).

At φ = 0.3, these two equations give τ = 4.24 and 2.17, respectively. Because KC with τ= 2.50 matches the laboratory Rudies data at φ = 0.3, let us modify equations 10 and 11 so that both produce τ= 2.50 at φ= 0.3. These equations thus modified become, respectively,

$$\tau = 0.590\varphi^{-1.2}, \quad \ldots \quad (12)$$

and

$$\tau = 0.576(1+\varphi^{-1}) \quad \ldots \quad (13)$$

By substituting equations 12 and 13 into equation 9, we arrive at the following two KC estimates, respectively:

$$k = 0.0898\,\frac{D_0^2}{\varphi_0}\,\varphi^{4.4} \quad \ldots \quad (14)$$

and

$$k = 0.0942\,\frac{D_0^2}{\varphi_0}\,\frac{\varphi^4}{(1+\varphi)^2} \quad \ldots \quad (15)$$

with equation 14 giving the lower permeability estimate and equation 15 giving the upper estimate for porosity below 30%. For permeability in mD and pore diameter in mm, a multiplier 10^9 has to be added to the right-hand sides of these equations.

Finally, by introducing the percolation porosity into these equations and using the units mD for *k* and mm for D_0 , we obtain, respectively,

$$k = 0.0898\times 10^9\,\frac{D_0^2}{\varphi_0}\left(\varphi-\varphi_p\right)^{4.4} \quad \ldots \quad (16)$$

and

$$k = 0.0942\times10^{9}\frac{D_0^2}{\varphi_0}\frac{\left(\varphi+\varphi_p\right)^4}{\left(1+\varphi+\varphi_p\right)^2} \quad \ldots\ldots(17)$$

Other Permeability-Porosity Trends and Their Explanation

In most rocks, permeability does not follow the classic clay free trend equations 16 and 17. The question is then how to use the KC equation to explain or predict permeability in such formations. To address this question, we will use the KC functional form with the grain size d .

Let us now recall equation 3 and modify it to be used with k in mD and S in mm^{-1}:

$$k = \frac{10^9}{2}\frac{\varphi^3}{s^2\tau^2} \quad \ldots\ldots(18)$$

Assume next that the porosity evolution is due to mixing of two distinctively different grain sizes. The larger grain size is d_{SS} while the smaller grain size is d_{SH} and

$$d_{SH} = \lambda d_{ss}, \quad \ldots\ldots(19)$$

where: $\lambda < 1$ is constant.

Let the volume fraction of the smaller grains in the rock be C (we call it the shale content). Then, by following Marion's (1990) formalism and assuming grain mixing according to the ideal binary scheme (Figure 6), we obtain the total porosity φ of this mixture as shown:

$$\varphi = \varphi_{ss} - C(1-\varphi_{sh}) \quad \ldots\ldots(20)$$

for $C \leq \varphi_{ss}$, where φ_{ss} is the porosity of the large grain framework while φ_{sh} is that of the small grain framework.

Recalling now the expression for the specific surface area given earlier in the text, we obtain for the large grain framework (sand)

$$S_{ss} = {6(1-\varphi_{ss})}/{d_{ss}} \quad \ldots\ldots (21)$$

and for the shale

$$S_{sh} = {6(1-\varphi_{sh})}/{d_{sh}} \quad \ldots\ldots (22)$$

Assume next that the total specific surface area of the sand/shale mixture is the sum of the two, the latter is weighted by the shale content:

$$S = S_{ss} + CS_{sh} = \frac{6}{d_{ss}}[1 - \varphi_{ss} + C\,(1-\varphi_{ss})/\lambda] \quad \ldots\ldots (23)$$

Now, by using Equations 20 and 23 together with equation 18, we find:

$$k = \frac{10^9}{72}\frac{d_{ss}^2}{\tau^2}\frac{[\varphi_{ss} - C(1-\varphi_{sh})]^3}{[1-\varphi_{ss} + C(1-\varphi_{ss})/\lambda]^2} \quad \ldots\ldots (24)$$

As before, we can modify equation 24 to include the percolation porosity:

$$k = \frac{10^9}{2}\frac{(\varphi - \varphi_p)^3}{S^2\tau^2} = \frac{10^9}{72}\frac{d_{ss}^2}{\tau^2}\frac{[\varphi_{ss} - C(1-\varphi_{sh}) - \varphi_p]^3}{[1-\varphi_{ss} + C(1-\varphi_{ss})/\lambda]^2} \quad \ldots\ldots (25)$$

where the total porosity is, as before, $\varphi = \varphi_{ss}$-C(1- φ_{sh}).

Results and Discussion

An example of using equation (6) to mimic the Rudies clean sandstone data (Lala, 2003) as well as the sorted Matullah sandstone data obtained from Belayim marine field, Gulf of Suez, Egypt is shown in Figure 1. The laboratory techniques used for measuring the petrophysical parameters used in this study are presented in Lala and Nahla (2015). The curve in this figure is according to Equation 6 with d = 0.250 mm (for Rudies), τ = 2.5, and φ_p = zero, 0.01, 0.02, and 0.03. The grain size in the Matullah dataset varies between 0.115 and 0.545 mm.

The Figure 2 shows the permeability normalized by the grain size squared, d^2. The Rudies sand data trend retains its shape. However, the Matullah sand data now

form a distinct permeability-porosity trend which approximately falls on the KC theoretical curve. This fact emphasizes the effect of the grain size on the permeability in obtaining permeability-porosity trends for formations where d is variable, k / d^2 rather than k alone is the appropriate argument.

Notice that although Equation 6 with $\varphi_p > 0$ mimics the permeability-porosity behavior of Rudies Formation data at high and low porosity, it somewhat underestimates the permeability in the 0.10 to 0.20 porosity range. The $\varphi_p = 0$ curve matches the data for porosity above 0.10 but overestimates the permeability in the $\varphi <$ 0.10 range. This is why in this porosity range, Bourbie et al. (1987) suggested to use a higher power of φ (e.g., 8) instead of 3. To us, introducing a finite percolation porosity appears to be more physically meaningful. Still, no matter how we choose to alter the input parameters, it is important to remember that KC equation is based on highly idealized representations of the pore space and it is remarkable that it sometimes works (same has to be said about two other remarkable "guesses," Archie's law for the electrical resistivity and Raymer's equation for the P-wave velocity, both discussed in (Mavko and Nur, 1997; Mavko et al., 2009).

Also, by observing the pore-space geometry evolution in Rudies sandstone, one may conclude that the pore size is variable (Figure 3): the pores shrink with decreasing porosity. In such a reservoir, the predicted permeability would be perfect if we consider only the porosity (pore spaces) and grain size in prediction.

The resulting tortuosity from equations 12 & 13 plotted versus porosity in Figure 4 rapidly increases with decreasing porosity, especially so in the porosity range below 10%.

Let us assume that φ_o = 0.30, D_0 = 0.10 mm, and φ_p = 0.01. The respective curves according to the two equations 16 & 17 are plotted on top of the Rudies and Mutallah data in Figure 5.

The percolation porosity used here is different from 0.02 used in Equation 6. The reason is that the current value 0.01 in Equations 16 and 17 gives a better match to Rudies data in the lower porosity range.

Needless to say that, the concept of "pore size" is a strong idealization, same as the concept of "grain size." We introduced it here because it is more consistent with the KC formalism than the latter idealization. Practical reason for using the equations with pore size is that this parameter can be inferred from the mercury injection experiments or directly from a digital image of a rock sample.

Let us assume d_{SS} = 0.25 mm; τ = 2.5 (fixed); and $\varphi_{ss} = \varphi_{sh}$ = 0.36. The resulting theoretical permeability estimates from equation 24 are plotted versus porosity in Figure 6 for λ = 1.00; 0.10 ;and 0.01.

The curve for λ = 0.10 matches the sandstone of Kharita Member data trend, obtained from the Western Desert, Egypt, while that for λ = 0.01 matches the Bahariya Formation data trend (Lala & Nahla, 2015). The curve for λ = 1.00 matches the high porosity part of the Rudies Formation data trend.

The percolation porosity value only weakly affects the theoretical permeability curves in the high and middle porosity ranges. This is why in Figure 6 we only show curves with $\varphi_p = 0$.

Conclusion

The goal of this work is to explore permutations of the Kozeny-Carman formalism and derive respective equations. Although the idealizations used in these derivations are strong and sometimes lack internal consistency, the results indicate the

significant flexibility of this formalism. The variants of the KC equation shown here can explain the various permeability-porosity trends observed in the laboratory, sometimes within the framework of physical and geological reasoning. The predictive ability of these equations is arguable since the input constants are not necessarily a-priori known. Still, as in the case of bimodal mixtures, they can help with the quality control of the existing data and forecasting of the permeability-porosity trends in similar sedimentary textures.

Acknowledgments

The author is indebted to the Egyptian General Petroleum Corporation (EGPC) for the permission to publish these laboratory results. The author is also grateful to anonymous reviewers whose constructive comments helped to improve this manuscript.

References

Amir, M.S. Lala, 2003, Effect of Sedimentary Rock Textures and Pore Structures on Its Acoustic Properties, M.Sc. Thesis, Geophysics Department, Ain Shams University, Egypt.

Amir, M.S. Lala, and Nahla, A.A. El-Sayed, 2015, The application of petrophysics to resolve fluid flow units and reservoir quality in the Upper Cretaceous Formations: Abu Sennan oil field, Egypt, Journal of African Earth Sciences, 102.

Bernabé Y., Li M., Maineult A. (2010) Permeability and pore connectivity: a new model based on network simulations, J. Geophysical .Research 115, B10203.

Berryman, J.G., 1981, Elastic wave propagation in fluid-saturated porous media, Journal of Acoustical Society of America, 69, 416-424.

Blangy, J. P., 1992, Integrated seismic lithologic interpretation: The petrophysical basis, Ph.D. thesis, Stanford University.

Bourbie, T., O. Coussy, and B. Zinszner, 1987, Acoustics of porous media, Gulf Publishing Company.

Boving, T.B., and Grathwohl, P., 2001, Tracer diffusion coefficients in sedimentary rocks: correlation to porosity and hydraulic conductivity, Journal of Contaminant Hydrology, 53, 85-100.

Carman, P.C. 1937. Fluid flow through granular beds. Transactions, Institution of Chemical Engineers, London, 15: 150-166.

Katz,D. L., Lee, L. L., 1990, Natural gas engineering, New York, McGraw Hill.

Kozeny, J. 1927. Ueber kapillare Leitung des Wassers im Boden. Sitzungsber Akad. Wiss., Wien, 136 (2a): 271-306.

Garanzha, V. A., Konshin, V. N., Lyons, S. L., Papavassliou, D. V., and Qin, G., 2000, Validation of non-Darcy well models using direct numerical simulation, Chen, Ewing and Shi (eds), Numerical treatment of multiphase flow in porous media, lecture notes in physics, 552, Springer-Verlag, Berlin, 156-169.

Guppy, K. H., Cinco-ey, H. and Ramey, H. J., 1982, Pressure buildup analysis of fractured wells producing a high low rates, Journal of Petroleum Technology, 2656-2666.

Marion, D., 1990, Acoustical, mechanical and transport properties of sediments and granular materials, Ph.D. thesis, Stanford University.

Martins, J. P., Miton-Taylor, D. and Leung, H. K., 1990, The effects of non-Darcy flow in proposed hydraulic fractures, SPE 20790, proceedings of SPE Annual Technical conference, New Orleans, Louisiana, USA, Sept. 23-26.

Mavko, G., and Nur, A., 1997, The effect of a percolation threshold in the Kozeny-Carman relation, Geophysics, 62, 1480-1482.

Mavko, G., Mukerji, T., and Dvorkin, J., 2009, The rock physics handbook, Cambridge University press.

Strandenes, S., 1991, Rock physics analysis of the Brent Group Reservoir in the Oseberg Field, Stanford Rock Physics and Borehole Geophysics Project, special volume.

Yves, Gueguen; Victor, Palciauskas 1994. Introduction to the physics of rocks. Princeton University Press.

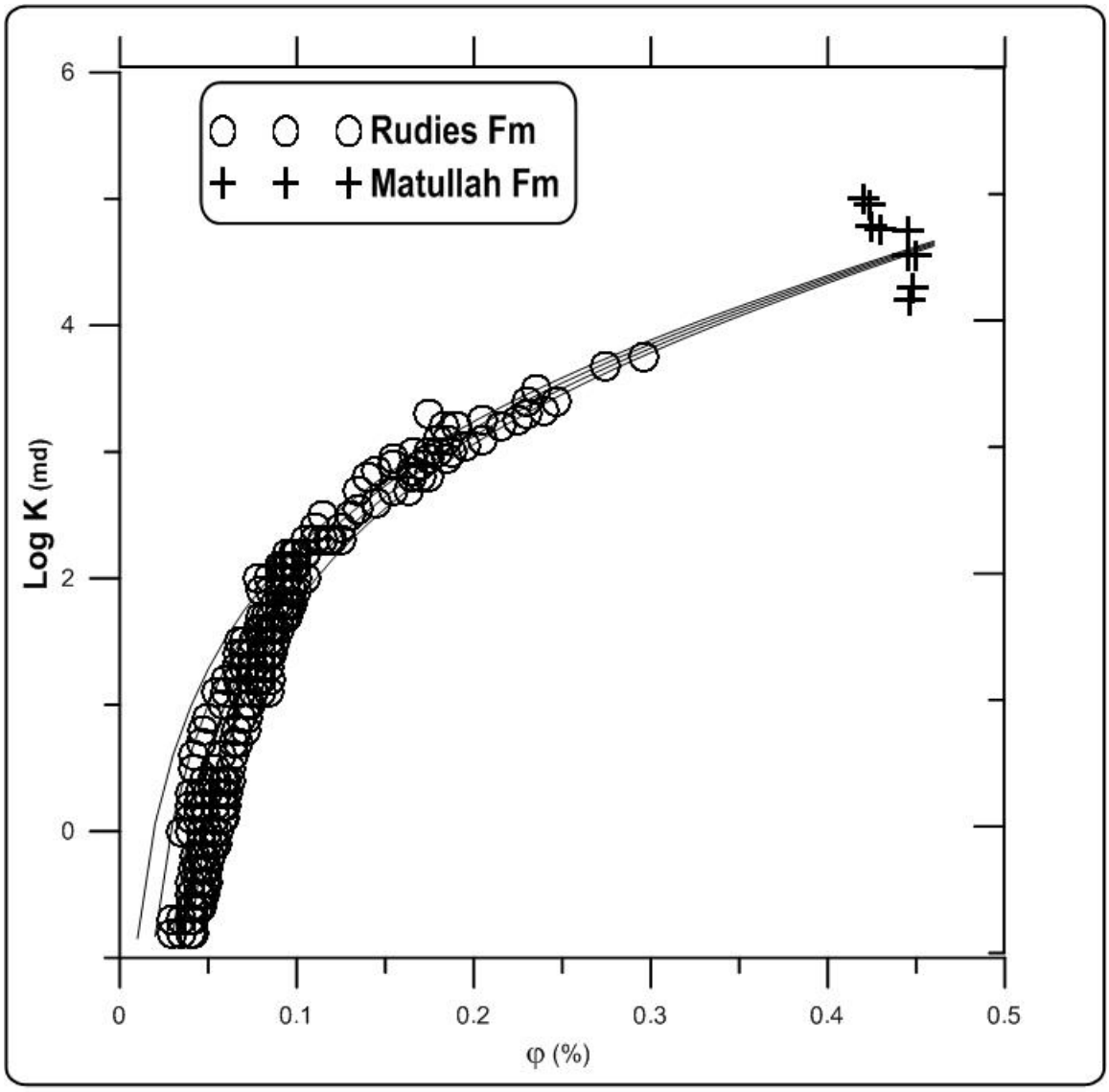

Fig.1.Porosity vs Permeability, the curves are from equation 6 with the percolation porosity (uppermost curve), 0.01, 0.02 and 0.03 (lowermost curve).

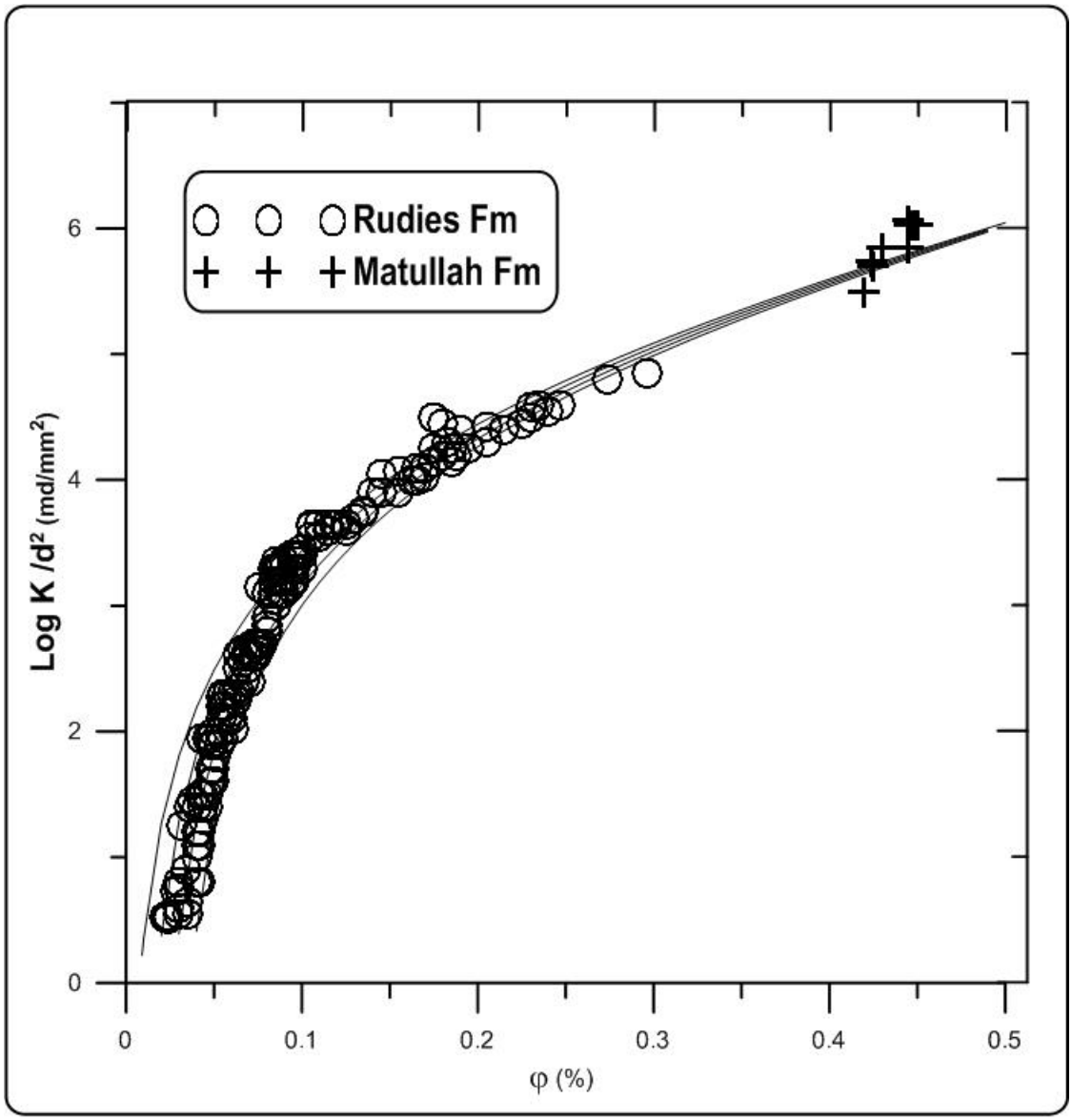

Fig.2.Porosity vs Permeability normalized by the grain size squared, the curves are from equation 6.

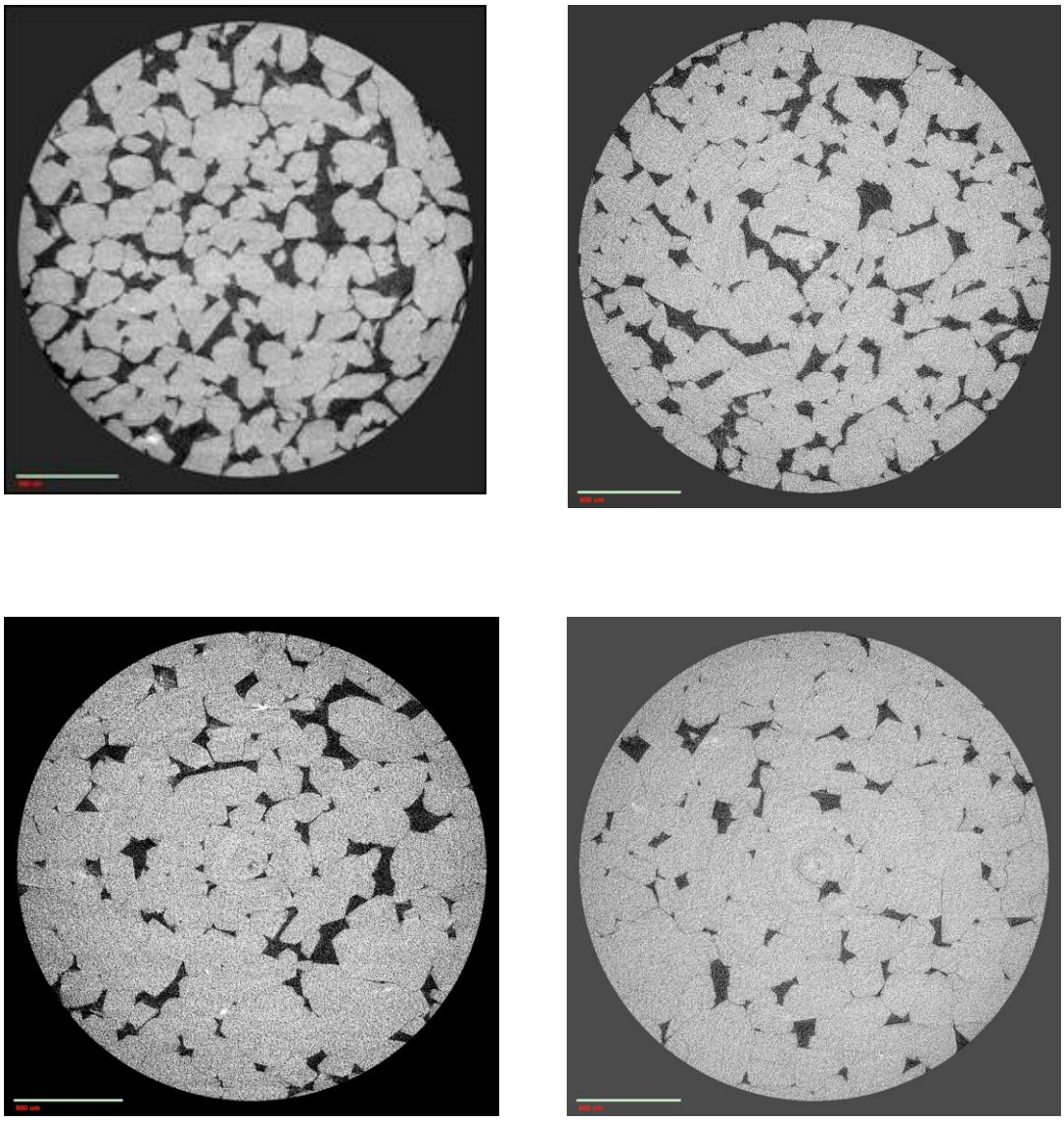

Fig.3. digital slice through four Rudies Fm samples whose porosity is gradually reducing (left to right and top to bottom). The scale barin each image is 500µm.

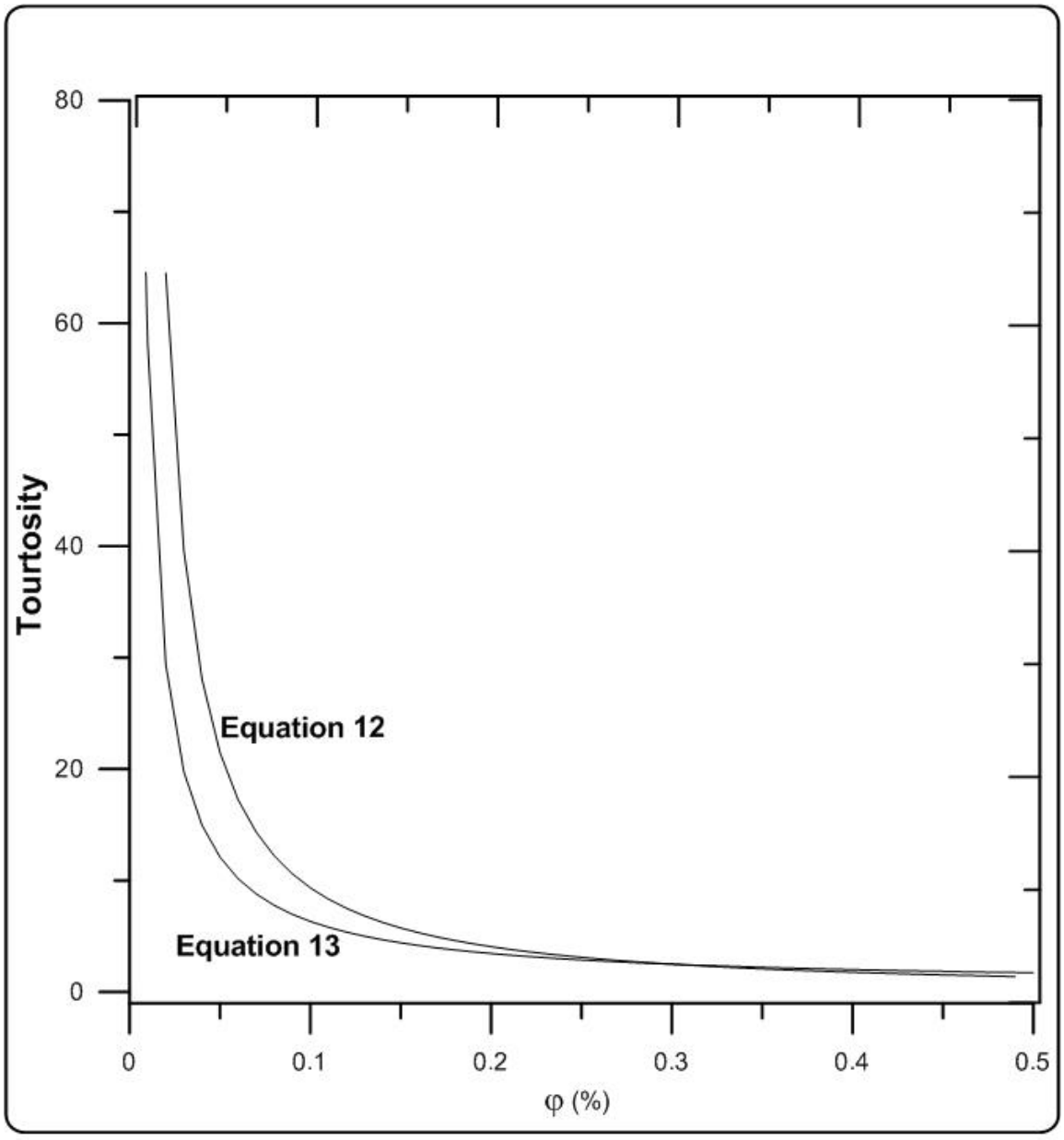

Fig.4. Porosity versus Tourtosity.

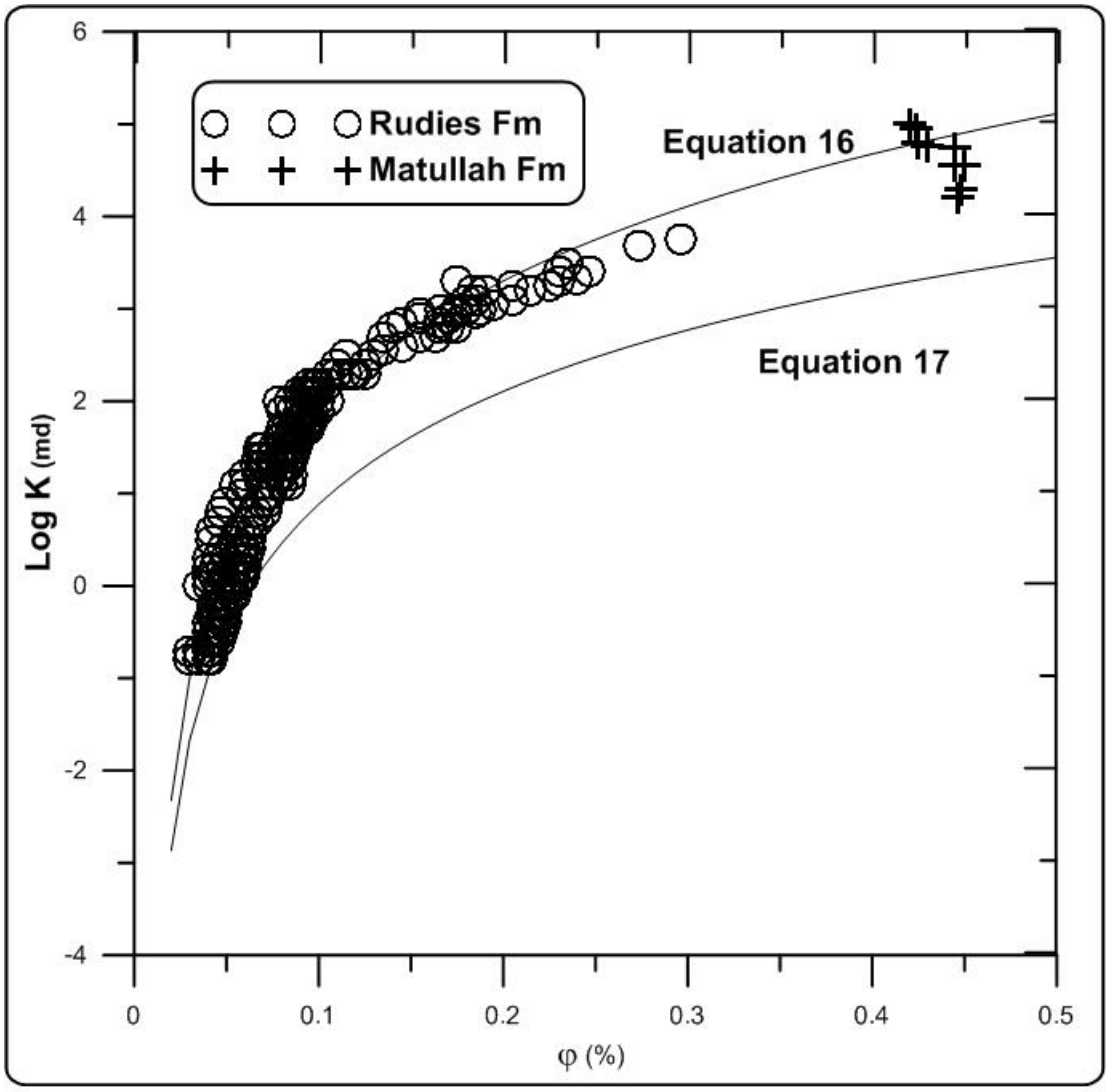

Fig.5.Porosity versus Permeability, curves are from equation 16 and 17.

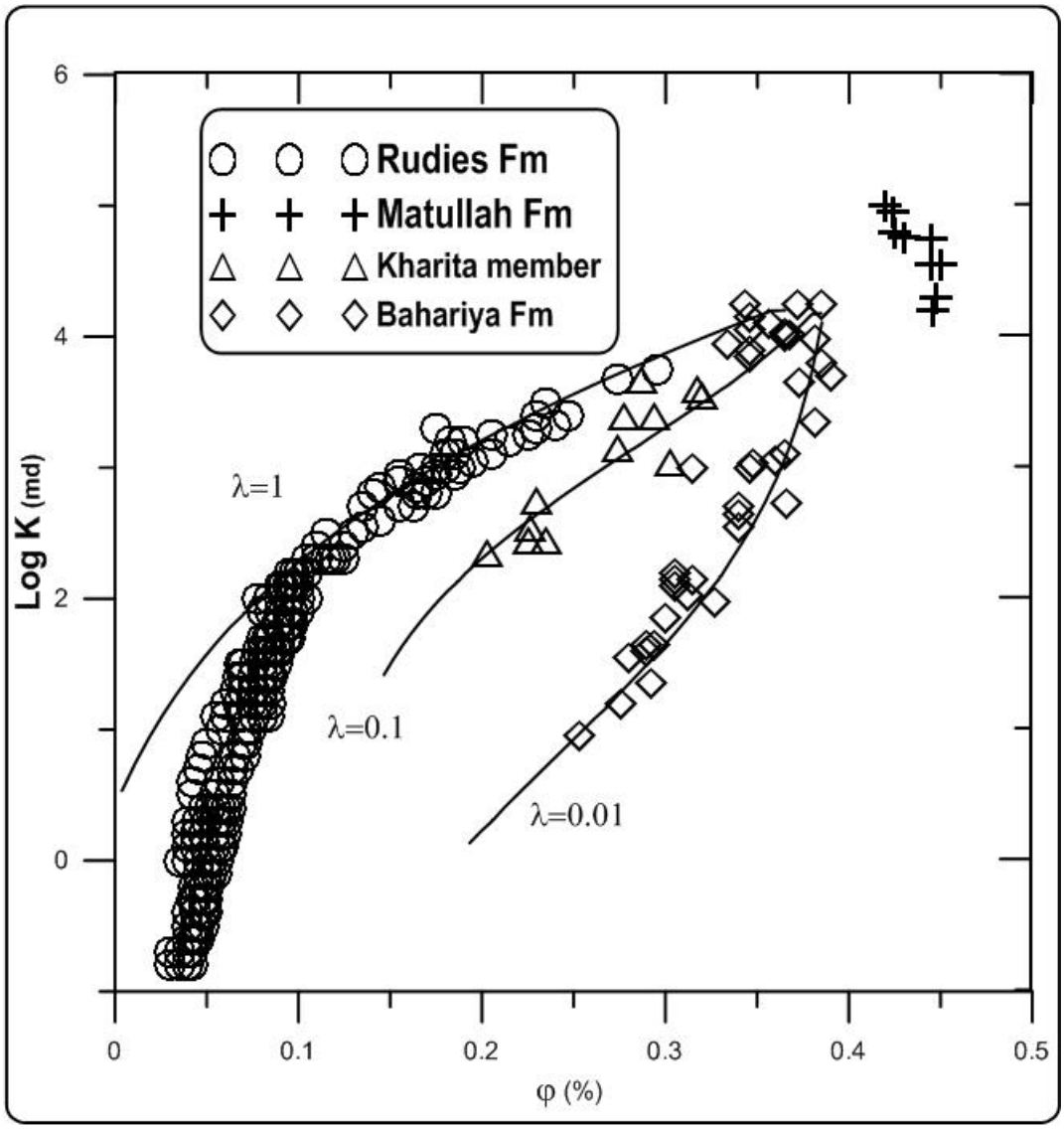

Fig.6.Porosity vs Permeability, the curves are from equation 24.

Table (1): Porosity and Permeability of the studied samples

No	Age	Depth (m)	Log Perm (md)	Porosity ratio	lithology
Well :113-81, Rudies Formation, Belayim land field, Gulf of Suez, Egypt					
1	Miocene	2578.2	-0.84	0.035	sandstone
2		2580.25	-0.72	0.035	sandstone
3		2722.31	-0.7	0.044	sandstone
4		2800.15	-0.56	0.044	sandstone
5		2476.64	-0.5	0.048	sandstone
6		2485.72	-0.31	0.05	sandstone
7		2491.68	-0.24	0.046	sandstone
8		N.A	-0.16	0.053	sandstone
9		N.A	-0.23	0.051	sandstone
10		N.A	-0.1	0.05	sandstone
11		N.A	0.11	0.049	Sandstone
12		N.A	0.27	0.048	Sandstone
13		N.A	0.29	0.055	Sandstone
14		2590.15	0.39	0.058	Sandstone
15		2599.54	0.55	0.054	Sandstone
16		2607.9	0.61	0.057	Sandstone
17		2612.86	0.75	0.064	Sandstone
18		2614	0.82	0.066	Sandstone
19		2620	0.94	0.072	Sandstone
20		2624.7	1.01	0.072	Sandstone
21		2639	1.14	0.076	Sandstone
22		2643.9	1.19	0.085	Sandstone
23		2661.05	1.3	0.076	Sandstone
24		2664	1.4	0.08	Sandstone
25		2688.32	1.75	0.085	Sandstone
26		2497.23	1.79	0.096	Sandstone
27		N.A.	1.9	0.094	Sandstone
28		N.A.	2	0.095	Sandstone
29		N.A.	2.12	0.096	Sandstone
30		N.A.	2.42	0.1	Sandstone
31		N.A.	2.63	0.118	Sandstone

Table (1, cont.) : Porosity and Permeability of the studied samples

No	Age	Depth (m)	Log Perm (md)	Porosity ratio	lithology
Well :113-81, Rudies Formation, Belayim land field, Gulf of Suez, Egypt					
32	Miocene	N.A	2.4	0.125	Sandstone
33		N.A	2.5	0.115	Sandstone
34		N.A	2.55	0.135	Sandstone
35		N.A	2.6	0.145	Sandstone
36		N.A	2.7	0.155	Sandstone
37		N.A	2.8	0.17	Sandstone
38		N.A	2.85	0.145	Sandstone
39		N.A	2.9	0.155	Sandstone
40		N.A	2.95	0.185	Sandstone
41		N.A	3	0.18	Sandstone
42		N.A	3.1	0.18	Sandstone
43		N.A	3.05	0.195	Sandstone
44		N.A	3.2	0.215	Sandstone
45		N.A	3.3	0.175	Sandstone
46		N.A	3.32	0.24	Sandstone
47		N.A	3.4	0.23	Sandstone
48		N.A	3.5	0.235	Sandstone
49		N.A	3.68	0.274	Sandstone
50		N.A	3.75	0.296	Sandstone

Table (1, cont.) : Porosity and Permeability of the studied samples

No	Age	Depth (m)	Log Perm (md)	Porosity ratio	lithology
Well :BED 1-2, Kharita member, Burg El Arab Formation, Western Desert, Egypt					
207		N.A.	2.45	0.225	Sandstone
208		N.A.	2.55	0.226	Sandstone
209		N.A.	2.45	0.235	Sandstone
211		N.A.	2.75	0.23	Sandstone
212		N.A.	3.15	0.274	Sandstone
214		N.A.	3.4	0.277	Sandstone
217		N.A.	3.4	0.294	Sandstone
218		N.A.	3.68	0.287	Sandstone
220		N.A.	3.05	0.303	Sandstone
221		N.A.	3.55	0.32	Sandstone
222		N.A.	3.6	0.317	Sandstone

Table (1, cont.) : Porosity and Permeability of the studied samples

No	Age	Depth (m)	Log Perm (md)	Porosity ratio	lithology
Well :BED 1-2, Bahariya Formation, Western Desert, Egypt					
1	Upper Cretaceous	N.A.	0.066	0.18	sandstone
2		N.A.	0.145	0.19	sandstone
3		N.A.	1.22	0.33	sandstone
4		N.A.	1.30	0.34	sandstone
5		N.A.	0.223	0.2	sandstone
6		N.A.	1.39	0.35	sandstone
7		N.A.	1.56	0.37	sandstone
8		N.A.	0.301	0.21	sandstone
10		N.A.	0.453	0.23	sandstone
11		N.A.	0.53	0.24	sandstone
13		N.A.	0.68	0.26	sandstone
14		N.A.	0.75	0.27	sandstone
15		N.A.	0.83	0.28	sandstone
16		N.A.	0.97	0.3	sandstone
17		N.A.	1.76	0.39	sandstone
18		N.A.	1.85	0.4	sandstone
19		N.A.	1.97	0.41	sandstone
20		N.A.	2.1	0.42	sandstone
21		N.A.	2.22	0.43	sandstone
22		N.A.	1.14	0.32	sandstone
23		N.A.	2.36	0.44	sandstone
24		N.A.	2.52	0.45	sandstone
25		N.A.	2.71	0.46	sandstone
26		N.A.	2.92	0.47	sandstone
27		N.A.	3.2	0.48	sandstone
28		N.A.	3.57	0.49	sandstone

Table (1, cont.): Porosity and Permeability of the Studied Samples

No	Age	Depth (m)	Log Perm (md)	Porosity ratio	lithology
Well :BM-85, Matullah Formation, Belayim marine field, Gulf of Suez, Egypt					
1	Lower senonian, upper cretaceous	3446.03	4.2	0.446	Sandstone
2		3449.03	4.3	0.448	Sandstone
3		3451.14	4.55	0.445	Sandstone
5		3455.17	4.75	0.445	Sandstone
7		3457.44	4.79	0.425	Sandstone
9		3473.45	4.95	0.424	Sandstone
10		3477.23	5	0.42	Sandstone

Dear editor,

We all appreciate your work and the comments from reviewers, and those comments are really helpful to improve the quality of this manuscript and our related research. Now we resubmit the revised version of this MS titled: "**Modifications to Kozeny-Carman Model to Enhance Petrophysical Relationships** ".

RESPONSE TO REFEREE REPORT(S):

1)The derivation of KC formalism is based on flow through pipe having a circular cross section with radius R. The specific surface area S (defined as the pore surface area divided by sample volume) can be expressed in terms of equation 4.

$$\varphi = \pi r^2 l / AL = \pi r^2 / A \tau \ldots\ldots (3)$$

Where τ is the tortuosity (defined as the ratio of total flow path length to length of the sample) .

$$S = 2\pi r l / AL = 2\pi r \tau / A = 2\pi r^2 \tau / A \, 2/r = 2\varphi / r \ldots\ldots (4)$$

Equation 5 is exact for an ideal circular pipe geometry is presented as

$$k = \pi R^4 / 8A \, L/l = \pi R^4 / 8A\tau = \frac{1}{2}\frac{\varphi^3}{S^2\tau^2} \ldots\ldots (5)$$

A common extension of the KC relation for a circular pipe is to consider a packing of identical spheres of diameter d. Although this granular pore space geometry is not consistent with the pipe like geometry,

it is common to use the original KC functional form. This allow a direct estimate of the (S) in terms of the porosity.

2) Using the grain size and model of packing of identical spheres of diameter (d) with the formalism. Explore introducing the radius of circular pipe. The parameters of modified KC equs given in 14 to 17 provide the very important parameters (pore throat radius) controlling the fluid flow in low porosity tight formation. Classical Rudies data is a special case illustrate the good description of the permeability by the grain size idealization because its clean and well sorted formation. So it will give good fit for equ 2 and 16 because τ is zero but this assumption will not valid for other medium to tight ill sorted and clayey formations. Thus equ 25 is risen. Diameter of pores is measured by capillary pressure curves.

3) table is provided

Line 202 – 204 The laboratory techniques used for measuring the petrophysical parameters used in this study are presented in Lala and Nahla (2015).

4) Darcy's law is inadequate for representing high velocity fluid flow in porous media, such as near the well bore. When correlating the data for high velocity water flow through porous media, Forchheimer (1901) found that the relationship between pressure gradient an fluid velocity was no longer linear, as described by linear Darcy's flow. Forchheimer effect also known as non-Darcy effect is very important for describing additional

pressure drawdown due to high fluid flow rates (Katz and Lee, 1990). Non-Darcy behavior illustrate significant effect on well performance. Non-Darcy effect play important role on effective fracture conductivity and gas well productivity. The Non Darcy flow could reduce the effective fracture conductivity and gas production and this confirmed by previous work (Guppy et al., 1982; Matias et al., Granazha et al., 2000).

Traditionally, the KC equation relates the absolute permeability to porosity and grain size (d), this form is fit permeability versus porosity for data set from clean well sorted sandstone during such calculations the grain sized kept constant. One find two inconsistences in this approach, a) KC equation has been derived for a solid medium with pipe conduits rather than for a granular medium and b) even if grain size is used in this equation, it is not obvious that it doesn't vary with varying porosity. bearing this argument in mind, we explore how permeability can be predicted consistently within the KC formalism by varying the radii of the conduits. However this approach requires tourtosity evaluation during porosity reduction. Some arrive at alternate forms for the KC equation by varying tourtuosity which predict permeability and produce permeability that match measured lab data.

Line 48 and 51: I specify the industry Line 47

Line 53: Done (References)

Line 61: Done

Line 74: Done Line 85 to 87. The specific surface area is much more difficult to measure or infer from the porosity because the granular pore spaces geometry is not consistent with the pipe like geometry model of the original K-C functional form.

Line 75: Done line 87 to 91. One other parameter that can be determined in the laboratory by sieve analysis or optical microscope is the average grain size (diameter) d. The sieve analysis is the most easily understood laboratory method of determination where grains are separated on sieves of different sizes.

Line 80-81: Because the KC formalism is based on cylindrical pipe model not the spherical grain packing model so this is not consistent with the KC model. However, introducing the grain size diameter improve the relationship between the permeability and the porosity so it is useful.

Line 82: Done (spherical)

Line 87: Done (Reference) Line 102

Line 116: Rudies Data is provided in table, Done Line 129 to 131 the Rudies Formation data obtained from Belayim marine field, Gulf of Suez, Egypt and the respective theoretical curves according to equation 6 and presented in figures 1 and 2,

Line 119 to 124: Done

Line 134: equ 6 , figures 1 and 2 Done line 131

Line 137 to 144: I made test for these new equations to other published data which give good results. D and Do which determined from capillary pressure curves, this different work is send also for peer review

Line 155 to 157: it doesn't include the term of clay percentage λ

Line 206: citation done

Line 209 to 211: Done

Line 214 to 215: This is valid only for the ideal case of clean well sorted formation such as Rudies Formation, where the pore shrink with decreasing porosity.

Line 223: I argue that equs 16 and 17 gives a better match than equ 6 at the lower porosity range (Tight formations).

Line 225-229: The pore size concept is more consistent with the KC formalism than the grain size because it can describe permeability of tight formation at lower porosity range. Thus equations 16 and 17 give a better match at lower porosity range, also equ 16 gives a good job but overestimate permeability at high porosity but equs 6 and 24 include the grain size give poor work at lower porosity range (tight formation).

I appreciate for Editors/Reviewers' warm work earnestly, and hope that the correction will meet with approval. Once again, thank you very much for your comments and suggestions.